

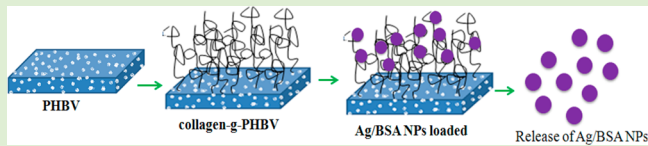
# Synthesis and Characterization of Collagen Grafted Poly(hydroxybutyrate–valerate) (PHBV) Scaffold for Loading of Bovine Serum Albumin Capped Silver (Ag/BSA) Nanoparticles in the Potential Use of Tissue Engineering Application

Rotimi A. Bakare, Chandra Bhan, and Dharmaraj Raghavan\*

Polymer Group, Department of Chemistry, Howard University, Washington, D.C. 20059, United States

## Supporting Information

**ABSTRACT:** The objective of this study is to synthesize and characterize collagen grafted poly(3-hydroxybutyrate-*co*-3-hydroxylvalerate) (PHBV) film for loading of BSA capped silver (Ag/BSA) nanoparticles. Thermal radical copolymerization and aminolysis methods were used to functionalize macroporous PHBV, followed by collagen grafting so as to formulate collagen-g-poly(hydroxyethylmethyl acrylate)-g-poly(3-hydroxybutyrate-*co*-3-hydroxylvalerate) [collagen-g-PHEMA-g-PHBV] and collagen-g-aminated-poly(3-hydroxybutyrate-*co*-3-hydroxylvalerate) [collagen-g-NH<sub>2</sub>-PHBV] films, respectively. Spectroscopic (FTIR, XPS), physical (SEM), and thermal (TGA) techniques were used to characterize the functionalized PHBV films. The amount of collagen present on grafted PHBV film was quantified by the Bradford method. The Ag/BSA nanoparticles were then loaded on collagen grafted and untreated PHBV films, and the nanoparticles loading were determined by atomic absorption spectrometry. The amount of nanoparticles loaded on collagen grafted PHBV film was found to be significantly greater than that on the untreated PHBV film. The nanoparticles loaded PHBV film can potentially serve as a scaffold to promote the growth of bone cells while inhibiting the bacterial growth.



## INTRODUCTION

Bacterial polyesters such as poly(hydroxyl alkonates) (PHAs) are biosynthesized from agricultural feedstocks by a variety of microorganisms (such as *Escherichia coli* strains) as intracellular energy and carbon storage materials.<sup>1</sup> The physical properties (high crystallinity, high melting point, strength, and modulus) of these polymers are generally comparable to that of isotactic polypropylene, with the exception of its brittle characteristics. Traditionally, the brittle characteristic of PHAs is addressed by incorporating monomers into the PHA backbone structure.<sup>2</sup> By adjusting the percent composition of 3-hydroxylvaleric acid (HV) content in the copolymer, mechanical properties, and degradation rates of PHBV have been modulated. For example, the degradation of PHBV (*in vivo*, 6 months) has been adjusted from 15% to 43% by varying the HV content of the copolymer.<sup>3</sup> Likewise, by adjusting the HV content of PHBV from 0 to 20%, the elasticity increases by about 180% of extension at break.<sup>4</sup> There have been additional reports to indicate that the mechanical properties of PHBV can be further tuned to attain or exceed the mechanical properties of cancellous bone (Young's modulus of 1 GPa, and tensile strength of 13 MPa).<sup>5–7</sup>

The combination of tunable mechanical properties and degradation rates along with nontoxicity of PHBV makes PHBV blends/composites a potentially attractive material for use in drug delivery system, medical implants, specialty packaging, and orthopedic devices. Additionally, PHBV displays a piezoelectric feature which makes it extremely beneficial for

use in bone tissue engineering.<sup>8</sup> Doyle et al. have demonstrated that implants based on PHB not only promote favorable bone tissue responses but also do not elicit inflammation after implantation for up to 12 months. Clinical studies of PHBV have shown that there is no malignant tumor formation in the region where PHBV is used as implant.<sup>6,9</sup>

Despite the desirable characteristics of PHBV for potential use in bone tissue engineering applications, the surface properties of PHBV are not ideal to support cell growth because of its inert and hydrophobic characteristics as well as lack of surface roughness. The cytocompatibility of PHBV can be improved by addressing the surface bioactivity of the polymer matrix.<sup>13–16</sup> An approach to increase the bioactivity of the matrix is to enhance the surface area of the polymer by formulating a porous 3D scaffold so as to facilitate cell anchoring and improved transfer of nutrients across the matrix.<sup>10,11</sup> Additionally, by modifying the polymer surface with biomacromolecules, i.e., extra cellular matrix proteins, the cell anchoring to polymer can be improved. Among the various extracellular matrix proteins, collagen in particular has received considerable importance because of its known ability to anchor the fibroblasts or epithelium cells.<sup>12</sup> For example, Tesema et al. reported that the collagen immobilized PHBV matrix provided a more favorable matrix for UMR-106 cell line proliferation (246%) than the unmodified PHBV matrix.<sup>13</sup> In a similar

Received: November 15, 2013

Published: December 12, 2013



manner, Baek et al. immobilized collagen on an amine treated PHBV/hydroxyapatite composite scaffold. Their results showed that the collagen immobilized composite scaffold possessed better osteoblast cell adhesion, proliferation, and differentiation (67%) compared to the untreated PHBV scaffold.<sup>14</sup> Additionally, Wang et al. reported a 244% increase in sheep chondrocytes cells viability and proliferation when cultured on a collagen immobilized PHBV scaffold relative to an unmodified PHBV.<sup>15</sup> Hu et al. also observed a similar trend in fibroblast cell growth on collagen immobilized PHBV scaffold: an increase of nearly 86% enhancement in cell proliferation compared to unmodified PHBV.<sup>16</sup> The rationale for this improvement is the presence of cell-binding domains containing the RGD (Arg-Gly-Asp) and DGEA (Asp-Gly-Glu-Ala) sequences in collagen that promote the interaction with the receptors present on the cell wall of adhering cells.<sup>17–19</sup>

Collagen can be immobilized on a PHBV matrix that has been functionalized by chemical or physical processes involving graft polymerization using oxygen plasma treatment, or UV-induced photografting, or  $\gamma$  irradiation, or ozone treatment.<sup>10,20–23</sup> Wang et al.<sup>24</sup> have previously reported the preparation of collagen grafted PHBV by initial treatment of NH<sub>2</sub>-PHBV scaffold with glutaraldehyde (GA) and subsequent collagen immobilization.

Despite the success in addressing the cytocompatibility of PHBV by immobilizing collagen, there are some serious concerns about infections by bacteria when PHBV film is used in joint arthroplasty.<sup>26</sup> The prevalent bacteria found in the infected region of joint replacement are *Staphylococcus aureus*, *Pseudomonas aeruginosa*, and *Escherichia coli*.<sup>27</sup> An approach recently sought to address the bacterial infection of PHBV film used in joint arthroplasty is to load the matrix with nanoparticles so that the nanoparticles upon release can maintain an aseptic environment in the neighborhood of the infections.<sup>26</sup> Among the various nanoparticles, silver nanoparticle has received prime consideration because it shows strong antimicrobial activity against a range of Gram-positive and Gram-negative bacteria at low concentration, while it exhibits cytotoxicity toward mammalian cells at a much higher concentration.<sup>28–30</sup> Flores et al. reported that Ag nanoparticles exhibited inhibitory effects toward *S. aureus* and *P. aeruginosa* at concentration less than 4  $\mu\text{M}$  while cytotoxicity toward the UMR-106 cell line was observed only at Ag nanoparticles concentration above 50  $\mu\text{M}$ .<sup>31</sup> The concentration window (between 4 and 50  $\mu\text{M}$ ) could be effectively used to design nanoparticles loaded matrix that upon its release in the physiological medium could maintain a sterile environment against microorganisms without cytotoxicity effects.

Recently, Xing et al. investigated the potential use of nanoparticles loaded PHBV nanofibers for joint arthroplasty application, where the nanoparticles were physically embedded in the PHBV nanofibers for maintaining a sterile environment.<sup>26</sup> Here, we conjugate the nanoparticles with proteins so as to improve its biocompatibility, maintain stability of nanoparticles over a wide range, and promote specific interaction between protein capped silver nanoparticles and collagen of collagen immobilized PHBV scaffold in formulating Ag/BSA nanoparticles loaded collagen grafted PHBV scaffold. Furthermore, the BSA of Ag/BSA nanoparticles was used to promote electrostatic interaction with collagen of collagen immobilized PHBV film so as to retain the nanoparticles on

collagen grafted PHBV film as established by our recent findings on model substrate.<sup>34,35</sup>

To the best of our knowledge, synthesis of collagen immobilized PHEMA grafted PHBV scaffold and formulation of Ag/BSA nanoparticles loaded collagen grafted PHBV scaffolds have not been previously reported. The formulation of nanoparticles loaded PHBV matrix based on electrostatic interaction is novel and can be potentially useful in the triggered release of nanoparticles from the matrix based on the pH, ionic strength of the medium, and other physiological factors near the region of interest.

Here, we use established procedures to functionalize porous PHBV films with amine and hydroxyl groups.<sup>24,36</sup> Next we have attached linker groups to functionalized PHBV films so as to graft collagen on the functionalized PHBV films. We have used spectroscopic (<sup>1</sup>H NMR, FTIR, XPS), physical (SEM), chemical (ninhydrin), and thermal (TGA) analytical techniques to characterize the functionalized PHBV films. The density of collagen grafted on PHBV films was quantified by Bradford assay. The collagen immobilized PHBV films and untreated PHBV films (control substrates) were immersed in Ag/BSA nanoparticle solution (4 °C, pH 7.4), and the amount of nanoparticles loaded was determined by atomic absorption spectrometry (AAS) using digested nanoparticle samples. We observed that the amount of nanoparticles loaded on collagen grafted PHBV films was significantly greater than that on the untreated PHBV films.

## EXPERIMENTAL SECTION

**Materials.** Poly(3-hydroxybutyrate-co-3-hydroxyvalerate) (PHBV) containing 12 wt % of hydroxyl valerate (HV), 2-hydroxyethyl methacrylate (HEMA), benzoyl peroxide (BPO), carbonyldiimidazole (CDI), Bradford reagent, and Type 1 collagen were purchased from Sigma-Aldrich. Chloroform and glutaraldehyde (GA) were purchased from Alfa Aesar. 1,6-Hexanediamine was purchased from Acros Organics. Ethanol was obtained from Fisher Scientific. All chemicals were used as received without further purification.

**Preparation of Porous PHBV Films.** A combination of solvent casting and solute leaching technique was used in the preparation of macroporous PHBV films. Sodium chloride was crushed using mortar and pestle and sieved to obtain particles of size 75–150  $\mu\text{m}$ . 2 g of sieved NaCl was manually mixed with 2 g of PHBV. 20 mL of CHCl<sub>3</sub> was added to the NaCl/PHBV mixture, and the slurry was heated at 60 °C for 2 h to make 10% w/v (0.1 g/mL) solution. The resulting solution was poured in a Petri dish and covered with perforated aluminum foil at room temperature for 24 h so as to allow the gradual evaporation of the solvent from the solution. The film was retrieved from the Petri dish and vacuum-dried overnight to remove the traces of solvent. Dried films were cut into 1 cm<sup>2</sup> size and washed with large amounts of deionized water until the filtrate was free of chloride ions, as determined by the addition of silver nitrate to the filtrate. The resulting porous films were vacuum-dried to constant mass at room temperature.

**Activation of Porous PHBV Films.** Porous PHBV films were immersed in 1,6-hexanediamine solution prepared in 2-propanol (12% w/v) at 37 °C for 40 min.<sup>38</sup> After 40 min, the films were removed and washed with deionized water for 24 h to remove free 1,6-hexanediamine and dried to constant mass at room temperature. The ninhydrin method was used to quantify the amine content in PHBV films.

Alternatively, porous PHBV films were functionalized by adopting the procedure reported by Lao et al.<sup>36</sup> for graft polymerization of PHEMA on PHBV films. The porous films were placed in a Schlenk flask containing 50 mL of 0.2 M HEMA solution purged with nitrogen for 30 min. To the contents in the flask, 2 mL of 0.0187 M BPO in acetone was added to initiate the radical polymerization at 80 °C

under a nitrogen atmosphere. After 4 h of reaction, the films were recovered and washed in hot ethanol for 3 h to remove unreacted HEMA and loosely bound homopolymer (PHEMA) from functionalized PHBV films. The grafted films were dried overnight under vacuum at 40 °C to obtain constant mass film. The grafting of PHEMA on PHBV films was characterized by FTIR, TGA, and NMR techniques, and the grafting density was established by differential mass gain analysis.

**Preparation of Collagen Immobilized PHBV Films.** To immobilize collagen on functionalized PHBV films, NH<sub>2</sub>-PHBV films were immersed in 1% w/v GA solution in deionized water for 3 h at 25 °C. The films were recovered and washed in deionized water overnight to remove unreacted GA. The GA activated NH<sub>2</sub>-PHBV films were then placed in collagen solution (3 mg/mL, in 0.5% acetic acid) for 24 h at 4 °C.

PHEMA-g-PHBV films were initially placed in 0.02 M CDI solution prepared in 1,4-dioxane at 37 °C for 2.5 h in water bath. The CDI treated films were then rinsed several times with 1,4-dioxane, followed by washing with deionized water to remove unreacted CDI from the film. The CDI-activated PHEMA-g-PHBV films were then immersed for 24 h in collagen solution (3 mg/mL, in 0.5% acetic acid) maintained at 4 °C.

The collagen immobilized scaffolds prepared using NH<sub>2</sub>-PHBV and PHEMA-g-PHBV films were washed for 72 h in 1% acetic acid to remove physically immobilized collagen. Subsequently, the films were dried, and collagen content was quantified by Bradford assay.

**Loading of Ag/BSA Nanoparticles on Collagen Immobilized PHBV Films.** The synthesis and characterization of Ag/BSA nanoparticles have been conducted in our laboratory, and details of the work can be found elsewhere.<sup>37</sup> Briefly, Ag/BSA nanoparticles were prepared by chemical reduction of the AgNO<sub>3</sub> and BSA mixture. The size of the nanoparticles was found to be 10–15 nm. The collagen immobilized PHBV films (collagen-g-PHEMA-g-PHBV) were immersed in 8 ppm Ag/BSA nanoparticle solution (freshly prepared stock solution was diluted in HEPES buffer of pH 7.4) for 2 h at 4 °C. The films were retrieved and gently washed to remove any loosely adhering nanoparticles. The washed solution and the residual solution after retrieval of films were combined and saved for fluorescence spectroscopy measurement. The gently washed films were subjected to extensive washing in 1 L of deionized water for 12 h with constant regular agitation to remove the physically entrapped Ag/BSA nanoparticles on the scaffolds. Care was taken to periodically replace the wash solution to effectively remove the physisorbed nanoparticles. The washed films were dried to a constant mass and saved in the desiccator for further analysis. The amount of nanoparticles bound to the washed films was assayed by digestion of the film followed by AAS measurement. Several trials with the nanoparticles adsorbed films were performed using similar loading and washing protocol to check the reproducibility of the technique (*t* test was performed on the data collected). A similar procedure was used to quantify the nanoparticles loaded on collagen-g-NH<sub>2</sub>-PHBV film. Macroporous PHBV films without collagen immobilization served as the control for nanoparticle loading study. Also, the nanoparticles loaded collagen grafted PHBV films were assayed by the XPS technique.

**Characterization. Fourier Transform Infrared–Attenuated Total Reflectance (FTIR-ATR).** FTIR spectra were recorded on Spectrum 100 FTIR spectrometer (PerkinElmer), equipped with a universal attenuated total reflection (UATR) accessory, LiTaO<sub>3</sub> detector, and KBr beam splitter. The spectra of porous PHBV films, NH<sub>2</sub>-PHBV, PHEMA-g-PHBV, collagen-g-NH<sub>2</sub>-PHBV, and collagen-g-PHEMA-g-PHBV films were collected in ATR mode with a resolution of 4 cm<sup>-1</sup>. A total of 128 scans were collected to ensure a good signal-to-noise ratio.

**Scanning Electron Microscopy (SEM).** Grafted, activated, and untreated porous PHBV films were mounted on an aluminum stub; gold metal was deposited on the films so as to enhance the sample conductivity. The films were observed using Jeol JSM 7600F field emission SEM. A 20 kV accelerating voltage and secondary electron mode along with a working distance of 8 mm were used for the morphological characterization of film. Micrographs were collected at

several magnifications so as to map the porosity and roughness of the film as a function of various treatment conditions.

**Thermogravimetric Analysis (TGA).** 8–12 mg of functionalized PHBV film was heated from room temperature to 550 °C at a heating rate of 20 °C/min and then cooled back to room temperature at a rate of 20 °C/min under a nitrogen atmosphere at a purge rate of 100 mL/min using TG/DTA 320 (Seiko Instruments Inc.). For comparison purposes, a thermogram of pure PHBV film was also recorded under similar conditions.

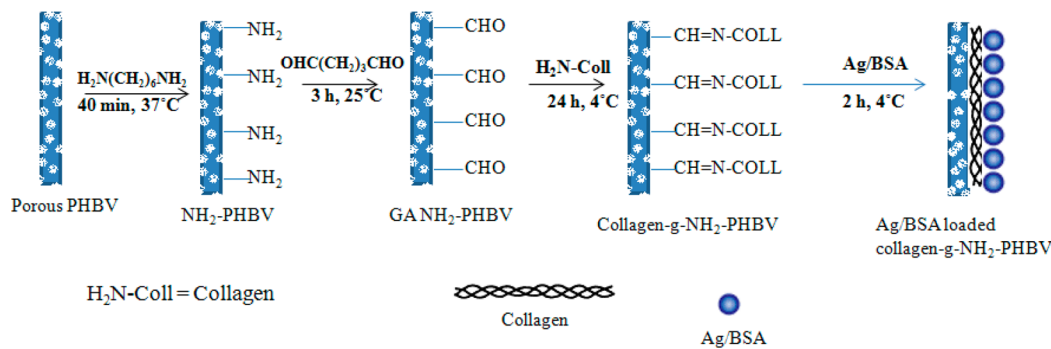
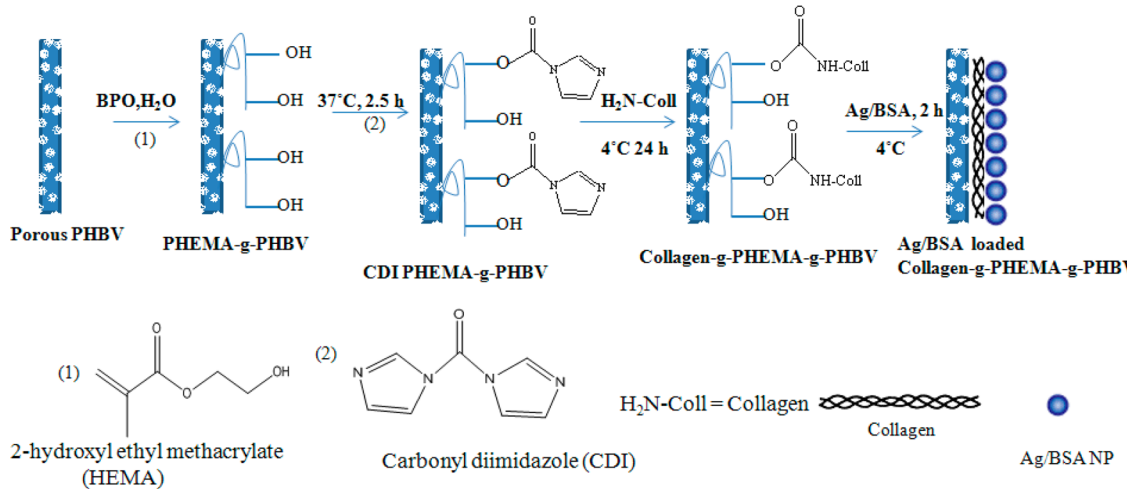
**Determination of the Amino Groups on NH<sub>2</sub>-PHBV Films.** The amount of amino groups formed on the aminolyzed porous PHBV (NH<sub>2</sub>-PHBV) films was determined by ninhydrin assay as described by Zhu et al.<sup>38</sup> The films were immersed in 1.0 M ninhydrin solution (in absolute ethanol) for 1 min in a test tube and heated for 15 min at 80 °C to promote reaction between ninhydrin and the amino groups of the NH<sub>2</sub>-PHBV film. Upon reaction, the surface of the NH<sub>2</sub>-PHBV films turned blue. After the evaporation of the adsorbed ethanol, 5 mL of 1,4-dioxane was added to dissolve the films. Another 5 mL of 2-propanol was added to stabilize the blue compound. The absorbance of the solution was recorded from 450 to 650 nm using an HP 8453 845x UV-vis system, Agilent Technologies. Standard solutions of 1,6-hexanediamine (0.31, 0.63, 1.25, 2.50, and 5.00 mM) were prepared and reacted with ninhydrin in 1,4-dioxane/isopropanol (in ratio 1:1, v:v) solution to obtain the absorbance v/s concentration calibration curve of standard solution. To obtain the amine content present in the films, the recorded absorbance of the NH<sub>2</sub>-PHBV film was compared with the absorbance against concentration calibration curve of standard solution. A similar protocol was used to measure the amine content in GA-treated PHBV films.

**Determination of Collagen Density on Collagen Grafted PHBV Films Using Bradford Assay.** Briefly, the collagen grafted films were placed in 6 M HCl for 2 h at 120 °C.<sup>39</sup> During acid treatment, the grafted collagen was hydrolyzed from the films and recovered. The pH of the solution was then adjusted to 7.0 by 6.0 M NaOH solution. To 0.1 mL of the neutralized solution, 5 mL of Coomassie brilliant blue solution was added and allowed to react for 10 min at 25 °C. The absorbance of the solution was then measured at 595 nm using a UV-vis spectrophotometer. The recorded absorbance was compared with calibration curve of standard collagen solution (10, 25, 50, and 100 µg/mL).

**XPS Characterization of PHBV Films.** The surface composition of porous PHBV, NH<sub>2</sub>-PHBV, collagen-g-NH<sub>2</sub>-PHBV, CDI-g-PHEMA-g-PHBV, collagen-g-PHEMA-g-PHBV, Ag/BSA loaded collagen-g-PHEMA-g-PHBV, and Ag/BSA loaded collagen-g-NH<sub>2</sub>-PHBV films was obtained with a Kratos Axis 165 X-ray photoelectron spectrometer, using monochromatic Al K $\alpha$  (1486.6 eV) X-ray source at 260 W. Charge neutralization was required to prevent surface charge buildup. Binding energies were charge corrected to 284.8 eV (NIST) for C 1s.

**Measurement of Ag/BSA Nanoparticles Loaded on Collagen Grafted PHBV Films.** To assay the silver content present on the nanoparticles loaded films, a digestion protocol recommended by US EPA was modified and used.<sup>40</sup> The films were acid digested in 20 mL of 2% v/v nitric acid at 165 °C for 25 min. An additional 5 mL of 2% v/v nitric acid was added and further digested for 15 min. The digested samples were allowed to cool to room temperature and diluted to a final volume of 25 mL with 2% v/v nitric acid. After centrifugation, supernatant was recovered and assayed by a graphite furnace atomic absorption spectrometer (AAS Analyst 800, PerkinElmer Precisely) at 328.1 nm. Standard solutions of Ag/BSA nanoparticles in the range of 0.75–12 ppb were prepared, acid digested, and assayed to obtain the calibration curve. Absorbance of the digested nanoparticles samples was compared with calibration curve to obtain information about the amount of nanoparticles loaded on the grafted PHBV films.

**Fluorescence Measurements.** Using a Shimadzu RF-5301PC spectrofluorometer, we collected the corrected fluorescence spectra of the BSA and nanoparticle solution before and after immersion of collagen immobilized PHBV samples. Water served as the blank for our measurement. The emission wavelength was recorded in the range of 315–500 nm with an excitation wavelength at 295 nm.

**Scheme 1. Synthesis Ag/BSA Nanoparticles Loaded Collagen-g-NH<sub>2</sub>-PHBV Films****Scheme 2. Synthesis of Ag/BSA Nanoparticles Loaded Collagen-g-PHEMA-g-PHBV Films**

Fluorescence spectra of the solution were collected in triplicate so as to establish data reproducibility.

## RESULTS AND DISCUSSION

Schemes 1 and 2 provide multistep reaction pathways to functionalize, graft collagen, and load nanoparticles on macroporous PHBV films. Briefly, during aminolysis (Scheme 1), one of the amino groups of 1,6-hexanediamine reacts with the ester group of PHBV to form an amide bond, leaving the other amino group of the hexanediamine available for further reaction.<sup>24,41,42</sup> On the other hand, during graft copolymerization of PHBV with HEMA (Scheme 2), it is believed that there is initial abstraction of the acidic protons from the backbone of PHBV chain to form macroradical and subsequent copolymerization of PHEMA grafts on PHBV backbone, leaving OH groups available for further reaction.<sup>36,43</sup> Since PHEMA-g-PHBV films can be degradable or nondegradable depending on the graft yield and NH<sub>2</sub>-PHBV film is degradable, we tested PHEMA-g-PHBV and NH<sub>2</sub>-PHBV films for loading nanoparticles in an attempt to prepare a degradable scaffold with loaded nanoparticles. Initially, the NH<sub>2</sub>-PHBV and PHEMA-g-PHBV films were activated and exposed to collagen solution. Subsequently, the collagen-g-PHBV films were exposed to nanoparticles solution. To establish whether the PHBV films were indeed functionalized during the multistep reaction pathway according to the schemes presented, FTIR, XPS, and TGA measurements were performed on the treated PHBV films and compared against pristine PHBV film.

Figure 1a shows the ATR-FTIR results of porous PHBV, PHEMA-g-PHBV, and collagen-g-PHEMA-g-PHBV films. In the FTIR of pure PHBV, we observe peaks at 2960 and 2920 cm<sup>-1</sup> corresponding to the methylene asymmetric and symmetric stretching, respectively. In addition, there is a sharp carbonyl stretching band at 1720 cm<sup>-1</sup> for the ester group in the pure PHBV film. Unlike IR of pure PHBV film, the ester peak in PHEMA-g-PHBV film at 1720 cm<sup>-1</sup> is very broad. The inset of Figure 1a shows the broad ester group spanning the region between 1760 and 1680 cm<sup>-1</sup>. The broad peak is because of the contribution from ester groups of PHBV (1720 cm<sup>-1</sup>) and PHEMA (1704 cm<sup>-1</sup>) from PHEMA grafted PHBV backbone.<sup>43</sup> Additional evidence for PHEMA grafting on PHBV was obtained from the IR peak at 3400–3100 cm<sup>-1</sup> (Figure 1a(ii)) which is commonly assigned to the hydroxyl group in a dried film. Figure S.1 provides supplemental data, i.e., <sup>1</sup>H NMR spectrum of PHEMA-g-PHBV sample dissolved in DMSO-d<sub>6</sub> to substantiate the PHEMA grafting of PHBV film. The characteristic peak for OH group was noticed at 4.8 ppm. Protons associated with the methyl and methylene groups of PHEMA were also noticed at 0.8, 1.8, 3.5, and 3.9 ppm. Also, proton peaks corresponding to methyl and methylene groups of the side chains and backbone of PHBV were observed in the <sup>1</sup>H NMR spectrum of the grafted sample. By use of differential mass % gain, we calculated the % of grafting yield, and it was found to be 45%.

Next, we studied the FTIR spectrum of the collagen-g-PHEMA-g-PHBV sample. We observed the broad absorption band around 3400 cm<sup>-1</sup> which can be assigned to the stretching

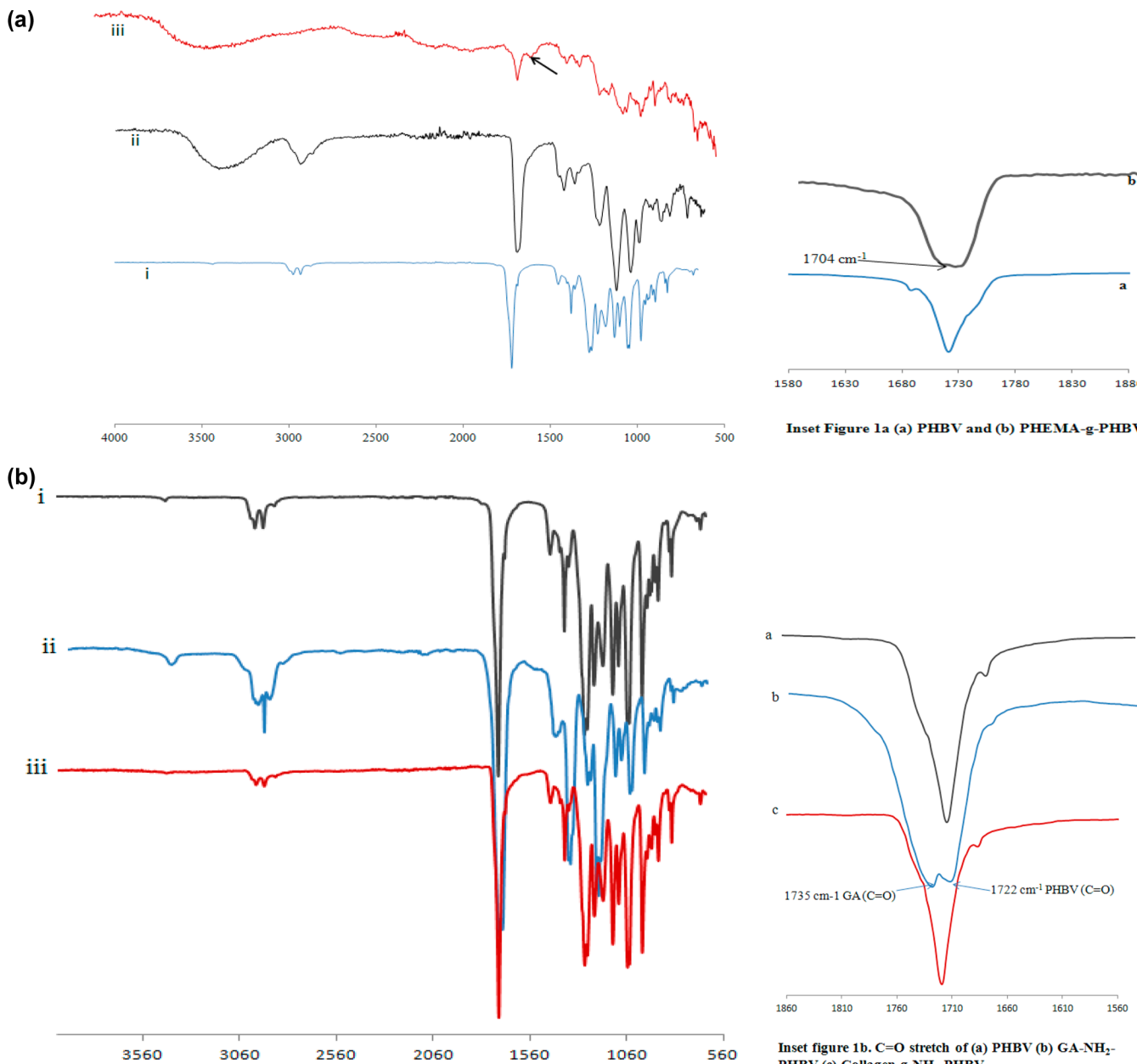


**Figure 1.** (a) FTIR spectra of (i) porous PHBV, (ii) PHEMA-g-PHBV, and (iii) collagen-g-PHEMA-g-PHBV films (arrow in (iii) indicates amide bond in collagen). (b) FTIR spectra (i), porous PHBV (ii), GA-NH<sub>2</sub>-PHBV (iii), and collagen-g-NH<sub>2</sub>-PHBV films.

vibration of O–H or N–H groups from grafted PHEMA or immobilized collagen macromolecule. Additionally, we noticed the emergence of a weak peak at 1648 cm<sup>-1</sup> (shown by the arrow in Figure 1a(iii)) which can be attributed to the amide I group in collagen. Additional supporting evidence for collagen grafting on PHEMA-g-PHBV sample was obtained from XPS and TGA measurements as well as Bradford assay.

Next, we investigated the GA activation of NH<sub>2</sub>-PHBV film and grafting of collagen on GA activated NH<sub>2</sub>-PHBV film. Figure 1b shows the FTIR spectra of PHBV, GA activated PHBV, and collagen-g-NH<sub>2</sub>-PHBV. In all the samples we observe peaks at 2960 and 2920 cm<sup>-1</sup> corresponding to the methylene asymmetric and symmetric stretching, respectively. In addition, there is a broad carbonyl stretching band from 1780 to 1680 cm<sup>-1</sup> in the GA activated NH<sub>2</sub>-PHBV film. The strong band from carbonyl group of aldehyde at 1735 cm<sup>-1</sup>

from glutaraldehyde appears to overlap with the carbonyl ester band of PHBV at 1720 cm<sup>-1</sup> (see inset). Upon immersion of GA activated NH<sub>2</sub>-PHBV film in collagen solution, we observe the disappearance of aldehyde carbonyl band, indicating the reaction of aldehyde functionality of GA with collagen. These observations were further supported by performing Bradford assay, XPS, as well as TGA measurements.

To establish whether there was indeed functionalization of PHBV film, thermograms and thermal stability data of functionalized film were compared with the untreated PHBV film. Figure 2a shows the thermogram of PHBV, PHEMA-g-PHBV, and collagen-g-PHEMA-g-PHBV film under a nitrogen atmosphere. The thermal stability of the polymer is commonly defined by parameters such as the onset decomposition temperature. The onset decomposition temperature ( $T_d$ ) is defined as the temperature at which known mass % of the

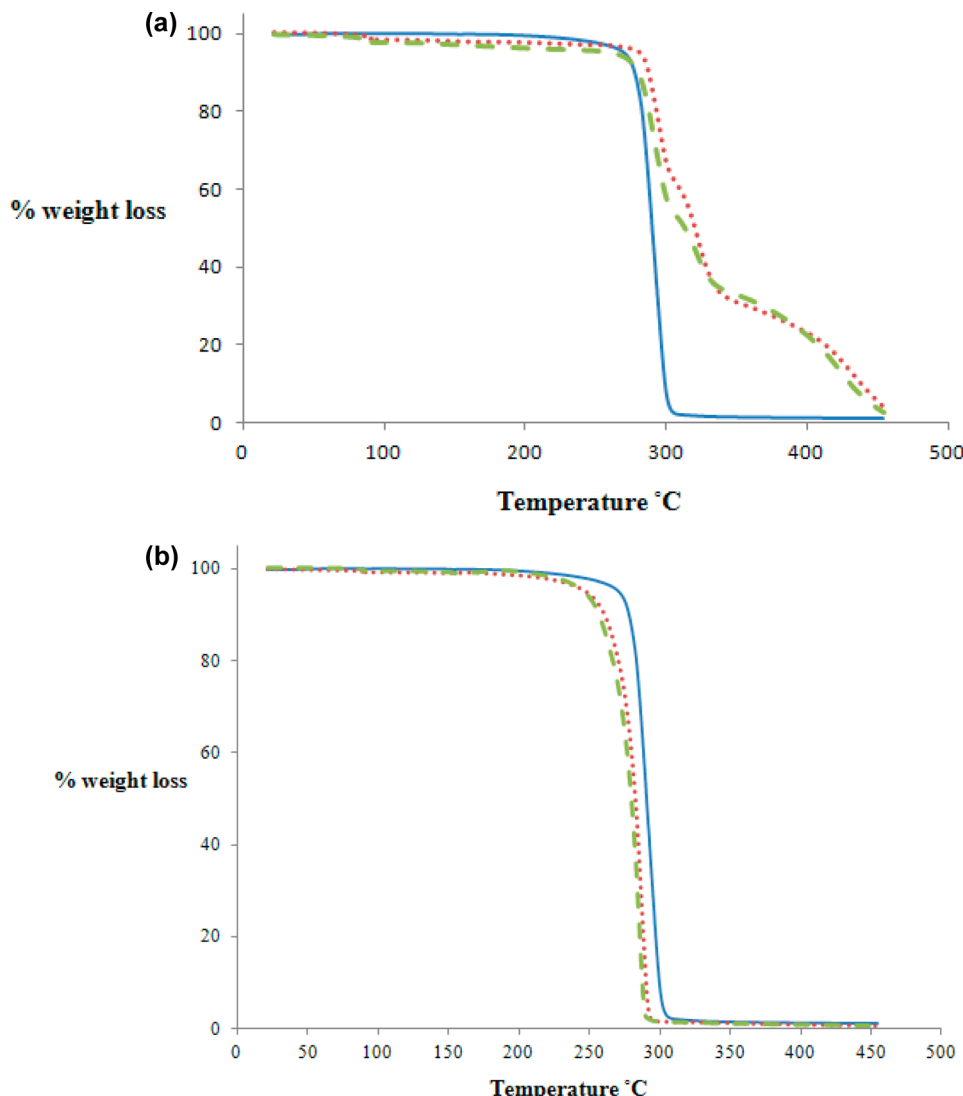


**Figure 2.** (a) Thermogravimetric analysis of PHBV (thick line), PHEMA-g-PHBV (dotted line), and collagen-g-PHEMA-g-PHBV (broken line) films. (b) Thermograms of PHBV (thick line), NH<sub>2</sub>-PHBV (dotted line), and collagen-g-NH<sub>2</sub>-PHBV (broken line) films.

sample is decomposed. Table 1 summarizes the thermal decomposition temperatures ( $T_{10\%}$ ) of PHBV film and functionalized PHBV film. Triplicate measurements were recorded for all the samples.

**Table 1. Decomposition Temperatures of PHBV and Modified PHBV Films**

sample	$T_{10\%}$ (°C)
porous PHBV	$263.15 \pm 0.35$
PHEMA-g-PHBV	$274.70 \pm 2.97$
collagen-g-PHEMA-g-PHBV	$264.60 \pm 1.20$
H <sub>2</sub> N-PHBV	$257.75 \pm 0.35$
collagen-g-NH <sub>2</sub> -PHBV	$256.15 \pm 1.06$

$T_{10\%}$  = temperature at 10% weight loss.

The thermogram of PHBV shows a one-step thermal degradation between 290 and 300 °C. Thermal degradation of PHBV is generally believed to proceed via random chain scission involving a formation of six-membered ring ester intermediate producing a carboxylic acid end group and an alkenyl end group.<sup>44,45</sup> On the other hand, the thermogram of

PHEMA-g-PHBV showed multiple steps, with the first step of degradation at 100 °C which can be attributed to the loss of entrapped moisture in the macroporous PHEMA-g-PHBV; followed by the degradation of PHBV between 310 and 320 °C (based on TGA results of pure PHBV), which is followed by the degradation of grafted PHEMA between 325 and 450 °C (based on the TGA results of pure PHEMA; data collected but not included), and the last step being the carbonization of polymer. A comparison of the TGA results indicates that there is a small improvement in the maximum decomposition temperature (~10 °C) of PHBV film upon grafting PHEMA on PHBV film. These results are consistent with several recent reports where grafting of PHEMA on PHBV has been shown to result in an increase in the onset decomposition temperature of PHBV film.<sup>42,43</sup> Like the PHEMA-g-PHBV film, in the thermogram of collagen-g-PHEMA-g-PHBV film, we observed multiple steps indicating that the PHEMA-g-PHBV matrix is indeed intact during collagen immobilization. Also, the thermal stability of the collagen-g-PHEMA-g-PHBV sample was nearly identical to the PHEMA-g-PHBV film where we observed nearly 10 °C improvement over pristine PHBV. This is because

collagen accounts for a negligible fraction of the grafted PHBV sample.

Figure 2b shows the thermogram of PHBV, NH<sub>2</sub>-PHBV, and collagen-g-NH<sub>2</sub>-PHBV film under a nitrogen atmosphere. When aminolysis was performed on porous PHBV film and subsequent collagen grafting was performed on the aminolyzed film, there was a small but significant drop in the onset decomposition temperature ( $\sim 7$  °C) of the functionalized films. A similar drop in the decomposition temperature of collagen-g-NH<sub>2</sub>-PHBV was also observed. The observed drop in onset decomposition temperature of PHBV films in NH<sub>2</sub>-PHBV and collagen-g-NH<sub>2</sub>-PHBV is probably because porous PHBV matrix facilitates improved diffusion of 1,6-hexamidine (a highly reactive chemical) across the matrix.<sup>24,25</sup>

SEM was used to assess the morphological changes of PHBV films before and after treatment and to establish that aminolysis treatment causes the degradation of PHBV films. Figure 3 is the

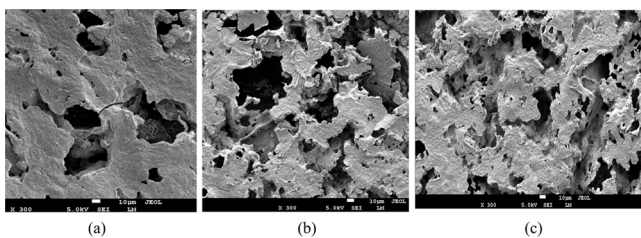


**Figure 3.** SEM of (a) PHBV, (b) NH<sub>2</sub>-PHBV, and (c) collagen-g-NH<sub>2</sub>-PHBV films.

SEM micrograph of PHBV, NH<sub>2</sub>-PHBV, and collagen-g-NH<sub>2</sub>-PHBV films. The PHBV films formed upon solvent casting and leaching of salt grains is rough. Leaching of salt grains introduces pores of the size of salt grains (nearly 100  $\mu\text{m}$ ) in the film and depending upon the weight percent of salt used in the formulation of macroporous PHBV film, a continuous pathway of pores across the film thickness can be generated. When the weight percent of leaching fraction in the salt/PHBV film exceeds the percolation threshold, an interconnected pathway is formed which facilitates diffusion of the reagent into and out of the bulk of the polymer. Clearly, the untreated film as observed by SEM undergoes significant change upon aminolysis and grafting. Compared to the untreated PHBV

surface (surface roughness 0.1983  $\mu\text{m}$ ), the NH<sub>2</sub>-PHBV film and collagen-g-NH<sub>2</sub>-PHBV film showed roughness of 0.2594 and 0.2643  $\mu\text{m}$ , respectively. Similarly, we noticed an increase in roughness of PHBV film due to PHEMA grafting and subsequent collagen immobilization (data available but not included) to macroporous PHBV film.

Further evidence about aminolysis of PHBV film was obtained by conducting ninhydrin assay of NH<sub>2</sub>-PHBV film. In Figure 4, we observed a peak with maximum absorbance at 558 nm for NH<sub>2</sub>-PHBV film corresponding to the blue reaction product.<sup>38</sup> As expected, we also noticed a peak at  $\lambda_{\max}$  of 558 nm for 1,6-hexamidine when complexed with ninhydrin solution. We related the absorbance recorded for the complex formed between NH<sub>2</sub>-PHBV and ninhydrin solution to the calibration curve obtained with 1,6-hexamidine, so as to quantify the amine content of the film. The amine content on NH<sub>2</sub>-PHBV film was found to be  $(4.53 \times 10^{-4} \pm 1.8 \times 10^{-4}$  mol/cm<sup>2</sup>) significantly greater than that reported previously for NH<sub>2</sub>-PHBV film ( $3.8 \times 10^{-7}$  mol/cm<sup>2</sup>) using a similar reaction condition.<sup>24</sup> The higher density of amine functionality in the treated PHBV film is probably a result of the use of macroporous PHBV film with enhanced surface area (cavity created in the PHBV film due to salt leaching) and possibly rougher sample. Also, by performing ninhydrin assay, we established the absence of amine functionality in GA treated NH<sub>2</sub>-PHBV film. Figure 4c shows no absorbance peak at 558 nm or blue coloration of the GA treated NH<sub>2</sub>-PHBV which suggests that the NH<sub>2</sub>-PHBV film has indeed reacted with GA.

The GA treated NH<sub>2</sub>-PHBV film was then immersed in collagen solution and then repeatedly washed so as to prepare collagen-g-NH<sub>2</sub>-PHBV film. The amount of collagen immobilized on collagen-g-NH<sub>2</sub>-PHBV film was determined by performing Bradford assay and by relating the absorbance of the solution against a standard calibration curve. As indicated in Table 2, the density of collagen grafted on collagen-g-NH<sub>2</sub>-PHBV film was found to be  $55.5 \pm 4.76$   $\mu\text{g}/\text{cm}^2$ , which was significantly greater than that previously reported by Wang et al. for a similar system ( $0.44 \mu\text{g}/\text{cm}^2$ ).<sup>24</sup> It must be noted that the film used in our study was macroporous as opposed to nonporous PHBV film as reported by Wang et al. The higher density of collagen in our film is primarily a result of higher amine incorporation during 1,6-hexamidine treatment which facilitates significant collagen immobilization. Also, we

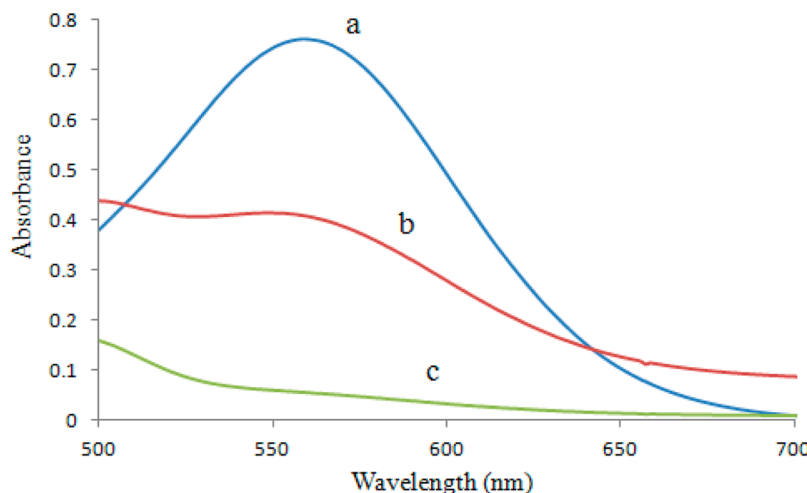


**Figure 4.** UV-vis measurements for ninhydrin assay of (a) 1,6-hexamidine, (b) NH<sub>2</sub>-PHBV, and (c) GA NH<sub>2</sub>-PHBV films at  $\lambda_{\max}$  558 nm.

**Table 2. Amine, Collagen, and Ag/BSA Nanoparticles Present on Modified and Unmodified PHBV Samples**

samples	amine conc ( $\times 10^{-4}$ mol/cm $^2$ )	collagen conc ( $\mu\text{g}/\text{cm}^2$ )	Ag/BSA loaded ( $\mu\text{g}/\text{cm}^2$ )
PHBV	NA <sup>a</sup>	NA	0.037 $\pm$ 0.011
NH <sub>2</sub> -PHBV	4.54 $\pm$ 1.08	NA	NA
collagen-g-NH <sub>2</sub> -PHBV	—	55.16 $\pm$ 4.76	0.29 $\pm$ 0.08
collagen-g-PHEMA-g-PHBV	—	29.93 $\pm$ 4.17	0.26 $\pm$ 0.06

<sup>a</sup>NA = not applicable.

quantified the density of collagen immobilized on collagen-g-PHEMA-g-PHBV and found it to be  $29.93 \pm 4.17 \mu\text{g}/\text{cm}^2$ . The higher amount of collagen on the collagen-g-NH<sub>2</sub>-PHBV film compared to the collagen-g-PHEMA-g-PHBV film is primarily a result of differences in the reactivity of cross-linking agents (GA and CDI) used to activate the film prior to collagen immobilization. A detailed discussion on this subject will follow in the subsequent sections.

XPS measurements were performed on treated PHBV films so as to substantiate our earlier findings that the films have been indeed functionalized and collagen was grafted on the PHBV films. Figure 5 shows the XPS survey spectra of PHBV, collagen-g-NH<sub>2</sub>-PHBV, and collagen-g-PHEMA-g-PHBV. Figure 6 is the curve fitting of high-resolution multiplex scan spectrum of C 1s region in pristine and functionalized PHBV films. The XPS survey scan of the salt leached porous PHBV film (Figure 5a) showed characteristic peaks of C 1s and O 1s at 284.8 and 532.8 eV, respectively. The ratio of carbon to oxygen (C/O) in the macroporous PHBV film was found to be

2.47, which was slightly higher than the calculated theoretical value of 2.25 based on the repeat units in PHBV. Our results are in general agreement with observations reported by Keen et al.<sup>41</sup> where it was reported that the C/O content in the pristine PHBV film is 2.65 as opposed to theoretical value of 2.25.

We observed four peaks (284.8, 286.4, 288.6, and 290.1 eV) in Figure 6a corresponding to the different chemical bonds (C–C/C–H, C–O, C(=O)–O, and COOH) of carbon in untreated PHBV film. Upon aminolysis of PHBV film with 1,6-hexanediamine, there was an emergence of N 1s peak at 399.5 eV in the survey spectrum (data available but not shown) amounting to 2.5% of the total content of the film which was considerably higher than the trace amount of N content in the pristine PHBV, which strongly supports amine functionality incorporation in the film. As reported previously, because of the use of macroporous PHBV film instead of nonporous PHBV film, the N content observed in our sample was higher than that reported by Wang et al.<sup>24</sup> (N content 1.6%). The successful incorporation of amine groups on PHBV film was further substantiated by carefully studying of the deconvoluted N 1s region of the NH<sub>2</sub>-PHBV sample. Figure 7 shows the high-resolution scan of N 1s region of NH<sub>2</sub>-PHBV, collagen-g-NH<sub>2</sub>-PHBV, CDI-PHEMA-g-PHBV, and collagen-g-PHEMA-g-PHBV. The four deconvoluted peaks of NH<sub>2</sub>-PHBV film have binding energies of 397.7, 399.4, 400.4, and 401.5 eV, which can be assigned to imine, amine, amide, and quaternary amine, respectively. This is in general agreement with the insertion step of 1,6-hexanediamine into PHBV film, where several reports have indicated that the reaction of amine with carboxylic acid or ester groups in PHBV leads to the formation of amide bonds.<sup>24,41,45</sup>

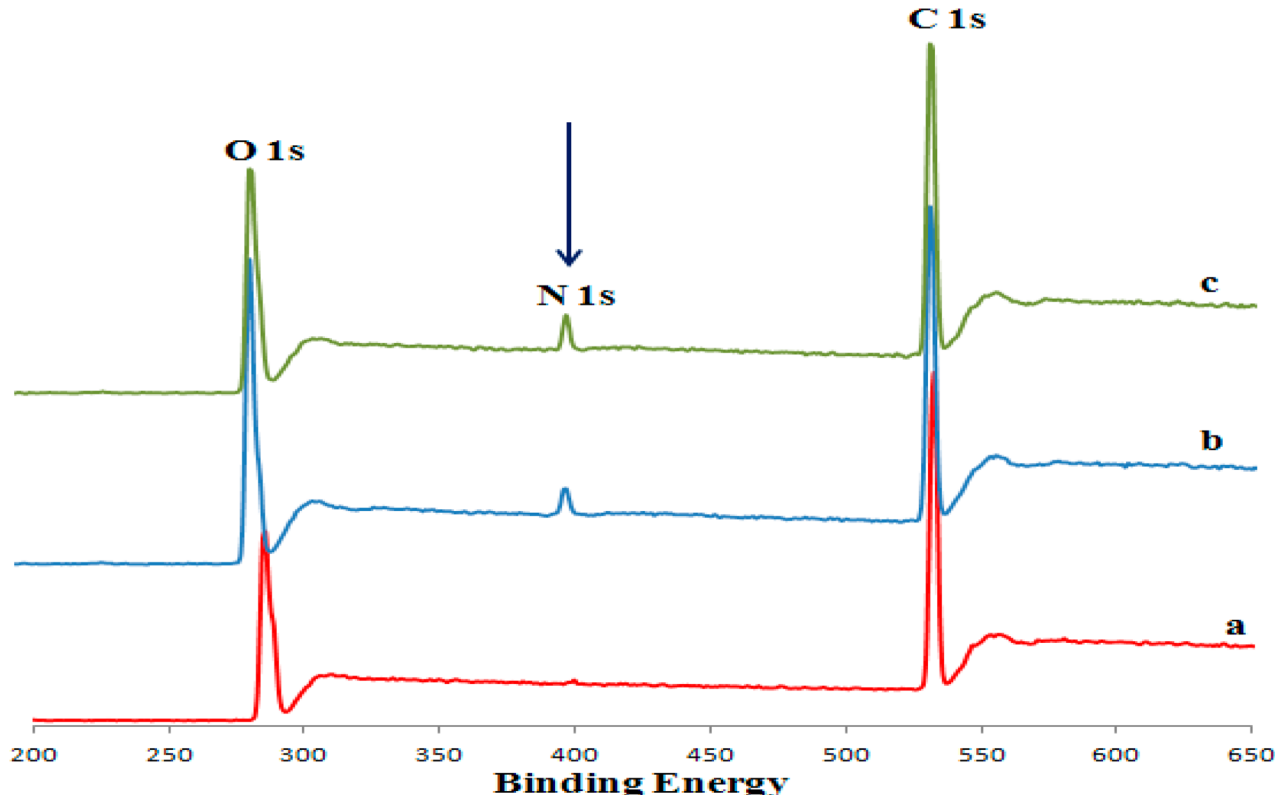


**Figure 5.** XPS survey spectra of (a) PHBV, (b) collagen-g-NH<sub>2</sub>-PHBV, and (c) collagen-g-PHEMA-g-PHBV films.

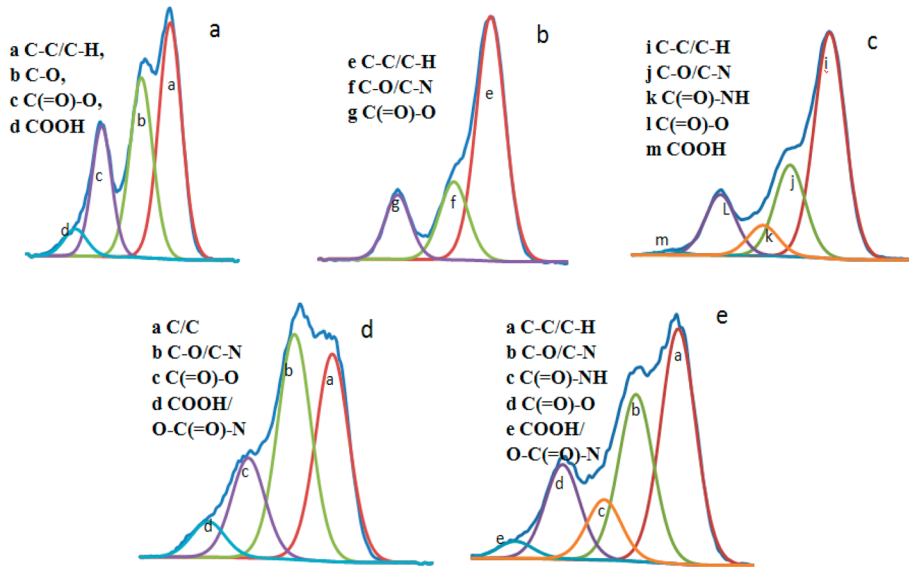


**Figure 6.** C 1s core level spectra of (a) PHBV, (b) NH<sub>2</sub>-PHBV, (c) collagen-g-NH<sub>2</sub>-PHBV, (d) CDI-PHEMA-g-PHBV, and (e) collagen-g-PHEMA-g-PHBV films.

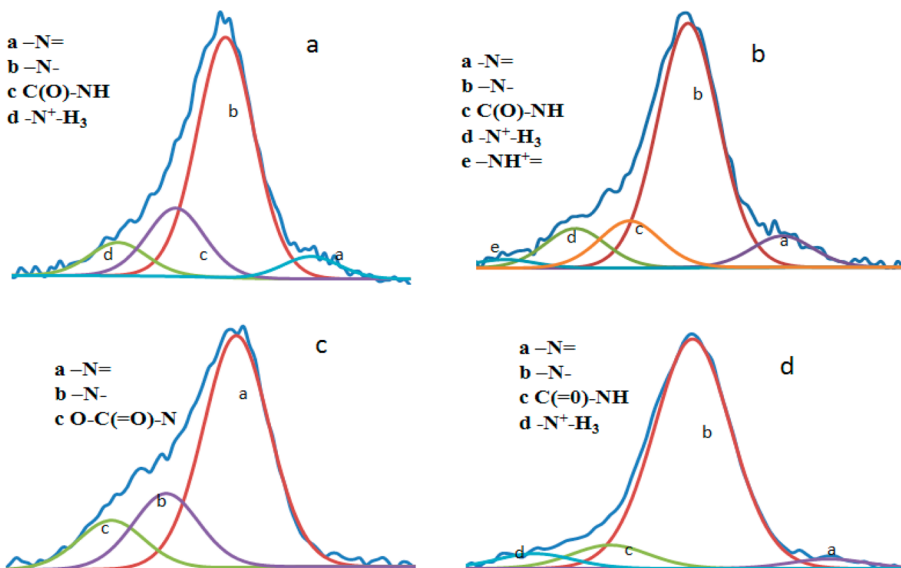


**Figure 7.** N 1s core level spectra of (a) NH<sub>2</sub>-PHBV, (b) collagen-g-NH<sub>2</sub>-PHBV, (c) CDI-PHEMA-g-PHBV, and (d) collagen-g-PHEMA-g-PHBV films.

The NH<sub>2</sub>-PHBV film was then subjected to GA treatment followed by collagen immobilization. Upon collagen immobilization, we observed further increase in the N content from 2.5% in NH<sub>2</sub>-PHBV to 3.0% in collagen-g-NH<sub>2</sub>-PHBV (see Figure Sb). The observed increase in the nitrogen content of the film can be a result of the nitrogen contribution from the immobilized collagen toward the overall N content of the film. The incorporation of collagen in NH<sub>2</sub>-PHBV film was substantiated by carefully studying the deconvoluted N region of functionalized PHBV sample. We noticed an additional peak in the deconvoluted N region corresponding to the protonated imine ( $-\text{NH}^+ = 403.1 \text{ eV}$ ),<sup>46</sup> which accounts for 3.69% of the total N content of the film. Previously, Manor et al., Hong et al., and Rodrigues et al.<sup>47–49</sup> have reported the formation of Schiff bases between GA, 1,6-hexanediamine, and primary amine of collagen at physiological pH, which is consistent with the

appearance of new protonated imine peak in the collagen-g-NH<sub>2</sub>-PHBV film.

Further evidence for collagen incorporation in the NH<sub>2</sub>-PHBV film was obtained by comparison of the deconvoluted region of the C 1s spectra of collagen-g-NH<sub>2</sub>-PHBV film and NH<sub>2</sub>-PHBV film, where we notice the reemergence of COOH peak in the collagen-g-NH<sub>2</sub>-PHBV film. The reemergence of COOH peak can be traced to the carboxylic acid functionality present in the grafted collagen macromolecule. Additionally, we observed the appearance of S 2p peak (164.8–168.7 eV) in the survey spectra of collagen-g-NH<sub>2</sub>-PHBV film which possibly could be related to the cysteine and methionine residues present in immobilized collagen (see Figure S2). Our XPS findings of functionalized PHBV film are consistent with aforementioned ninhydrin, FTIR, TGA, and Bradford assay results which confirms that 1,6-hexanediamine reacted with PHBV and collagen was indeed grafted on the NH<sub>2</sub>-PHBV film.

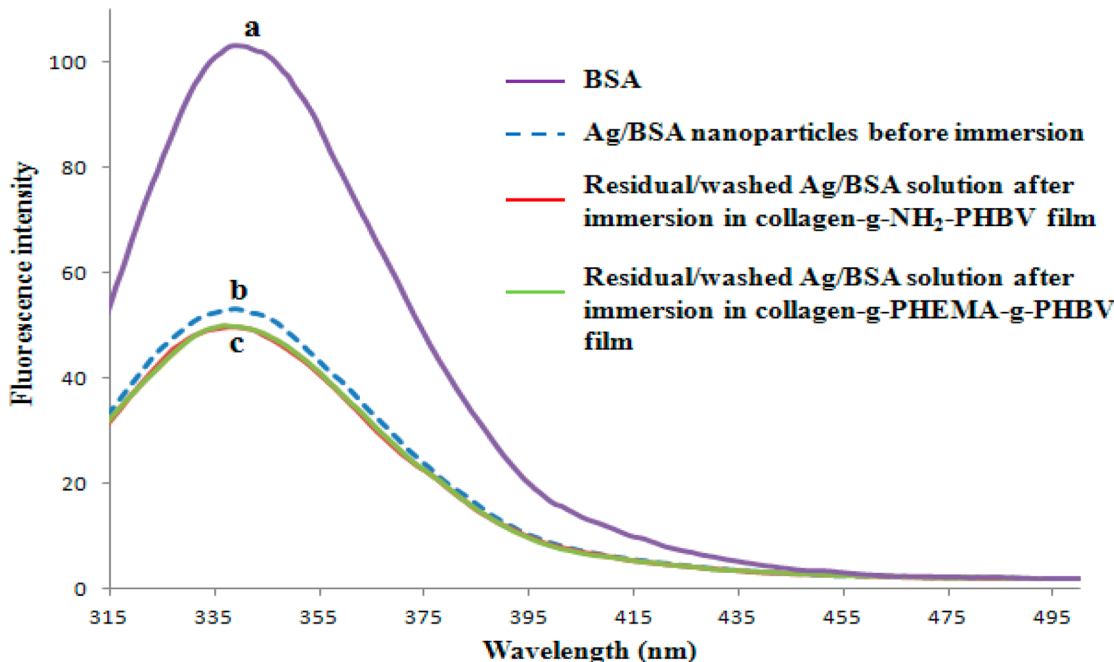


**Figure 8.** Fluorescence emission spectra of (a)  $0.48 \mu\text{M}$  BSA, (b) Ag/BSA nanoparticles before immersion, and (c) residual Ag/BSA solutions after immersion on collagen-g-NH<sub>2</sub>-PHBV and collagen-g-PHEMA-g-PHBV films.

To confirm that collagen was grafted on PHEMA-g-PHBV film, we carefully analyzed the deconvoluted C and N region of CDI activated PHEMA-g-PHBV film and collagen-g-PHEMA-g-PHBV film. The N 1s core-level spectrum (Figure 7c) showed imine, carbamate, and amine peaks<sup>50</sup> associated with CDI activated PHEMA-g-PHBV film. The functional groups introduced in CDI activated PHEMA-g-PHBV film is consistent with imidazole carbamate formation upon activation of the OH groups<sup>50–53</sup> on PHEMA-g-PHBV by CDI.

Several evidence from XPS results support the immobilization of collagen on CDI activated PHEMA-g-PHBV film. An increase in the overall N 1s content of collagen-g-PHEMA-g-PHBV (Figure 5c) was observed i.e. from 0.54% in pristine film to 3.8% in collagen grafted PHBV film. Additionally, we observed the appearance of amide peak in collagen-g-PHEMA-g-PHBV film (Figure 6e) which was not noticed in the CDI activated PHBV-g-PHEMA (Figure 6d). Furthermore, we observed S 2p peak (164.8–168.7 eV) in the survey spectra of collagen-g-PHEMA-g-PHBV film. The origin of S peak can be traced to the cysteine and methionine residue in collagen (Figure S2) of the collagen grafted PHBV-g-PHEMA system. On the basis of FTIR, NMR, TGA, and XPS results and Bradford assay, we have established that the PHBV film is grafted with PHEMA and collagen has been successfully immobilized on the PHEMA-g-PHBV film.

Next, the collagen grafted PHBV films and control (untreated) PHBV films were immersed in Ag/BSA nanoparticle solution of known concentration for 2 h. After gentle washing, the nanoparticles loaded films were saved for digestion and AAS measurement so as to quantify the nanoparticles present on the films. Qualitatively, to establish that the nanoparticles have been loaded on treated PHBV film, we performed fluorescence emission measurement of nanoparticle solution before and after immersion of film. Figure 8 shows the fluorescence emission spectra of BSA solution, Ag/BSA nanoparticle solution before immersion of film, and the residual solution after removal of film in combination with washed

solvent. For all the samples, the emission maxima appears at 340 nm, which is consistent with the emission spectral results reported for the BSA sample.<sup>54,55</sup> The decrease in the intensity of BSA upon conjugation with nanoparticles is a well-understood phenomena and is often referred to as the fluorescence quenching of protein upon its interaction with nanoparticles.<sup>54,55</sup> Additionally, in Figure 8, we observed a decrease in the fluorescence intensity of the nanoparticle solution upon the immersion of collagen grafted PHBV film. The decrease in the intensity of nanoparticle solution is purely a concentration effect, indicating that nanoparticles may have been loaded on collagen grafted PHBV film. It must be noted that the decrease in the fluorescence intensities of nanoparticle solution was observed for both grafted films upon loading of nanoparticles.

To establish that the recovered films have loaded nanoparticles, the recovered films were air-dried and then subjected to washing with large amount of deionized water ( $\sim 1 \text{ L}$ ) for 12 h so as to remove physisorbed and entrapped nanoparticles from the pores. Care was taken to replace the wash solution with fresh water at periodic intervals in order to achieve efficient removal of freely adsorbed nanoparticles from the film. The washed films were then subjected to digestion in 2%  $\text{HNO}_3$  solution for 30 min to extract the silver of the loaded Ag/BSA nanoparticles from the film into the solution. The silver content of the digested sample was determined using graphite furnace atomic absorption spectroscopy (GFAAS). As mentioned previously, in Table 2 the amount of the Ag/BSA nanoparticles loaded on collagen-g-NH<sub>2</sub>-PHBV and collagen-g-PHEMA-g-PHBV films is presented, and it was found to be  $0.29 \pm 0.08$  and  $0.26 \pm 0.06 \mu\text{g}/\text{cm}^2$ , respectively. On the other hand, a negligible amount of nanoparticles is loaded on untreated porous PHBV films. This is consistent with our expectation that the protonated amine functional groups of collagen on grafted PHBV film are involved in strong electrostatic interaction with the carboxylate anions of BSA of

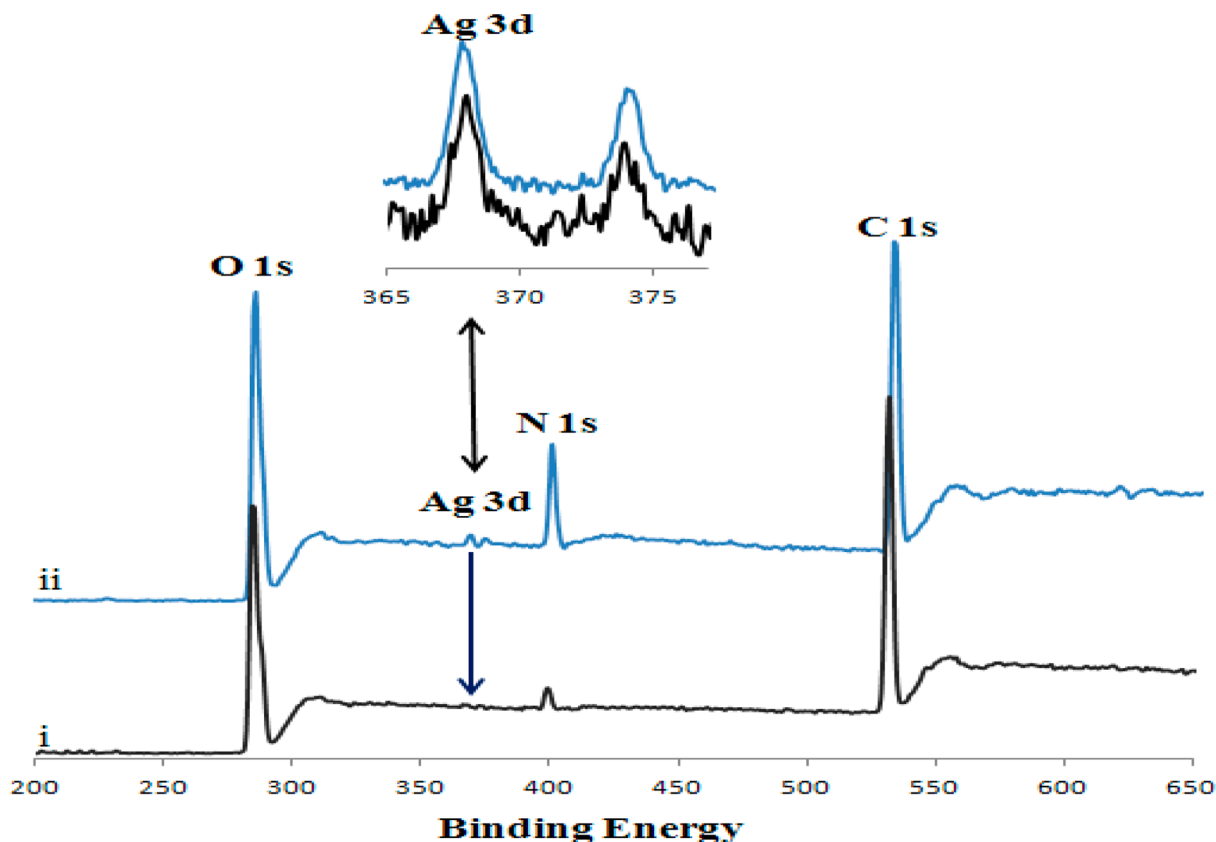


**Figure 9.** XPS survey spectra of Ag/BSA nanoparticles loaded on (i) collagen-g-NH<sub>2</sub>-PHBV and (ii) collagen-g-PHEMA-g-PHBV films.

nanoparticle solution,<sup>34,35</sup> and hence a significant amount of nanoparticles will be loaded on collagen grafted PHBV film.

Further confirmation of successful loading of Ag/BSA nanoparticles on the collagen grafted films was obtained by performing XPS analysis of washed Ag/BSA nanoparticles loaded PHBV films. Figure 9 shows the survey spectra of Ag/BSA nanoparticles loaded on collagen-g-NH<sub>2</sub>-PHBV and collagen-g-PHEMA-g-PHBV films. We noticed a sharp N peak in collagen-g-PHEMA-g-PHBV films which was not expected, and further studies are underway to evaluate the N buildup in the sample. More importantly, we noticed small Ag 3d peaks in the two systems (as shown by arrow). The inset showed the magnified Ag 3d region. This result complements our fluorescence and AAS results, indicating that Ag/BSA nanoparticles have indeed been loaded on macroporous collagen grafted PHBV films.

Next, we compared the two approaches used to immobilize collagen on functionalized PHBV films and nanoparticles loaded on immobilized collagen films. Table 2 compares the density of collagen immobilized on PHEMA-g-PHBV and NH<sub>2</sub>-PHBV sample. The NH<sub>2</sub>-PHBV sample showed higher collagen density than PHEMA-g-PHBV films. A possible explanation for the difference in the collagen density is the size difference of PHEMA and the 1,6-hexamidine. 1,6-Hexamidine is a small molecule compared to PHEMA macromolecule; hence, more aminated molecule may be grafted onto the PHBV film. Also, the activation by a short chain GA as opposed to bulky CDI molecule makes it more likely to build up higher density of GA activated NH<sub>2</sub>-PHBV than CDI activated PHEMA-g-PHBV. This may possibly explain the higher loading of collagen on GA activated film compared to CDI activated film.

Table 2 also compares the Ag/BSA nanoparticles loading on the collagen immobilized surfaces. We observed no significant difference (based on *t* test at 95% confidence level) in the amount of nanoparticles loaded on collagen-g-NH<sub>2</sub>-PHBV sample and collagen-g-PHEMA-g-PHBV sample despite significant differences in the collagen density grafted on the films. Bhan et al. demonstrated that at physiological pH the NH<sub>2</sub> functionality on self-assembled monolayer (SAM) or on immobilized collagen is important for Ag/BSA nanoparticles adsorption.<sup>34</sup> Despite high loading of collagen on GA activated PHBV film, since GA rapidly reacts with free primary NH<sub>2</sub> groups of collagen<sup>56</sup> and collagen can cross-link with multiple aldehyde site via lysine residues, a lesser amount of free amine groups may be available on collagen-g-NH<sub>2</sub>-PHBV film for nanoparticles loading. The proposed explanation is consistent with the Olde-Damink et al. observation where they noticed that within the initial 5 min of cross-linking with GA the amine group content in dermal sheep collagen decreased from 34/1000 amino acid residues to a plateau value of 5/1000 amino acids residues.<sup>56</sup> Also, our XPS results support the reduction in amine content of collagen-g-NH<sub>2</sub>-PHBV film. The reduction in primary amine content may offset the increased collagen density in collagen-g-NH<sub>2</sub>-PHBV film and hence the observed nearly identical nanoparticles loading on both collagens grafted films.

On the basis of our findings, we have successfully demonstrated that collagen grafted biocompatible PHBV film can serve as useful matrix to promote loading of Ag/BSA nanoparticles. Independent studies in our laboratory of Ag/BSA nanoparticles against *Escherichia coli* seem to suggest that at a threshold concentration of nanoparticles in physiological medium there may be inhibition of bacteria. The biological

studies need to be extended to Ag/BSA nanoparticles loaded on collagen grafted PHBV films so as to evaluate its antimicrobial efficacy. Future studies on nanoparticles loaded collagen grafted PHBV film, if successful, can provide a potential pathway to inhibit bacterial infection in joint anthropoplasty.

## CONCLUSIONS

The surface of the macroporous PHBV film was functionalized by two different methods, i.e. aminolysis and graft polymerization, so as to introduce amine groups and hydroxyl groups, respectively. Collagen was grafted on PHEMA-g-PHBV film with CDI as the cross-linking agent, while collagen was grafted on NH<sub>2</sub>-PHBV film with GA as the cross-linking agent. This was followed by the loading of Ag/BSA nanoparticles on collagen immobilized PHBV films. The functionalized PHBV film was characterized by FTIR, TGA, SEM, and XPS measurements. Several evidences point to collagen immobilization on PHBV film, such as the observation of characteristic amide peak in the FTIR spectrum, increase in the N content of the film noticed in the survey XPS spectra, increase in the film roughness based on SEM morphological data of treated film, and an increase in the collagen density of the film as measured by Bradford assay. The loading of nanoparticles on collagen-g-PHBV film was established qualitatively by fluorescence spectroscopy and quantitatively by atomic absorption spectroscopy. We noticed a decrease in the fluorescence intensity of the nanoparticle solution upon immersion of collagen grafted PHBV film in Ag/BSA solution, indicating that nanoparticles may be loaded on treated PHBV film. The nanoparticles loaded PHBV film and control PHBV film were acid digested, and silver content in the extract was measured by the AAS technique. Statistically, we noticed a negligible amount of nanoparticles loaded on untreated porous PHBV films while significant amount of nanoparticles were loaded on collagen grafted PHBV film (based on *t* test at 95% CL). This is possibly because of lack of functional groups present on untreated PHBV film to promote strong electrostatic interaction with the loaded nanoparticles, while the protonated amine functional groups of collagen on grafted PHBV film participate in strong electrostatic interaction with the carboxylate anions of BSA of nanoparticle solution.<sup>34,35</sup> Future studies will investigate the efficacy of Ag/BSA nanoparticles loaded collagen immobilized PHBV matrix in inhibiting bacterial infection when used for bone tissue engineering applications.

## ASSOCIATED CONTENT

### Supporting Information

Figure S.1 describes <sup>1</sup>H NMR spectrum of PHEMA-g-PHBV sample dissolved in DMSO-*d*<sub>6</sub> to substantiate the PHEMA grafting of PHBV film; the characteristic peak for OH group was noticed at 4.8 ppm; protons associated with the methyl and methylene groups of PHEMA were also noticed at 0.8, 1.8, 3.5, and 3.9 ppm; also, proton peaks corresponding to methyl and methylene groups of the side chains and backbone of PHBV were observed in the <sup>1</sup>H NMR spectrum of the grafted sample; Figures S2a and S2b show the core-level spectra of S 2p peak in collagen-g-NH<sub>2</sub>-PHBV and collagen-g-PHEMA-g-PHBV, respectively, which can be traced to the cysteine and methionine residue in collagen. This material is available free of charge via the Internet at <http://pubs.acs.org>.

## AUTHOR INFORMATION

### Corresponding Author

\*E-mail draghavan@howard.edu; Phone (+1) 202-806-4427 (D.R.).

### Notes

The authors declare no competing financial interest.

## ACKNOWLEDGMENTS

D. Raghavan acknowledges the financial support from NSF-MRSEC DMR-0820506. The authors also appreciate assistance from Surface Analysis Center at University of Maryland (UMD) in collecting XPS data. The authors thank Almaz Gebregeorgis from HU for assistance with synthesis and characterization of Ag/BSA NPs.

## REFERENCES

- (1) Jiang, L.; Chen, F.; Qian, J.; Huang, J.; Wolcott, W.; Liu, L.; Zhang, J. *Ind. Eng. Chem.* **2010**, *49*, 572–577.
- (2) Holmes, P. A. In *Development in Crystalline Polymers*; Bassett, D. C., Ed.; Elsevier Applied Science Publishers: London, 1988.
- (3) Gogolewski, S.; Jovanoic, M.; Perren, S.; Dillon, J. G.; Hughes, M. K. *J. Biomed. Mater. Res.* **1993**, *9*, 1135–1148.
- (4) Savenkova, L.; Gercberg, Z.; Bibers, I.; Kalnin, M. *Process Biochem.* **2000**, *36*, 445–450.
- (5) Hammond, T.; Liggett, J. J. *Degradable Polymers*; Scott, G., Gilead, D., Eds.; Chapman and Hall: New York, 1995.
- (6) Doyle, C.; Tanner, E. T.; Bonfield, W. *Biomaterials* **1991**, *12*, 841–847.
- (7) Lutton, C.; Read, J.; Trau, M. *Aust. J. Chem.* **2001**, *54*, 621–623.
- (8) Chen, G. Q.; Wu, O. *Biomaterials* **2005**, *26*, 6565–6578.
- (9) Shishatskaya, E. R.; Volova, T. G.; Puzyr, A. P.; Mogilnaya, O. A.; Efremova, S. N. *J. Mater. Sci.: Mater. Med.* **2004**, *15*, 719–728.
- (10) Kose, G. T.; Kenar, H.; Hasirci, N.; Hasirci, V. *Biomaterials* **2003**, *24*, 1949–1958.
- (11) Liu, H.; Raghavan, D.; Abegaz, S.; Stubbs, J. *J. Biomed. Mater. Res.* **2010**, *92*, 922–930.
- (12) Mauch, C.; Hatamochi, A.; Scharffetter, K.; Krieg, T. *Exp. Cell Res.* **1988**, *178*, 493–503.
- (13) Tesema, Y.; Raghavan, D.; Stubbs, J. *J. Appl. Polym. Sci.* **2005**, *98*, 1916–1921.
- (14) Baek, J.-Y.; Xing, Z.-C.; Kwak, G.; Yoon, K.-B.; Park, S.-Y.; Park, L. S.; Kang, I. K. *J. Nanomater.* **2012**, 1–11.
- (15) Wang, Y.; Ke, Y.; Ren, L.; Wu, G.; Chen, X.; Zhao, Q. *J. Biomed. Mater. Res.* **2009**, *88A*, 616–627.
- (16) Hu, S.-G.; Jou, C.-H.; Yang, M.-C. *Carbohydr. Polym.* **2004**, *58*, 173–179.
- (17) Anselme, K. *Biomaterials* **2000**, *21*, 667–681.
- (18) Rowley, J. A.; Madlambayan, G.; Mooney, D. J. *Biomaterials* **1999**, *20*, 45–53.
- (19) Chiang, T. M.; Kang, A. H. *J. Clin. Invest.* **1997**, *100*, 2079–2084.
- (20) Kose, G. T.; Ber, S.; Korkusuz, F.; Hasirci, V. *J. Mater. Sci.: Mater. Med.* **2003**, *14*, 121–126.
- (21) Shangguan, Y. Y.; Wang, Y. W.; Wu, Q.; Chen, G. Q. *Biomaterials* **2006**, *27*, 2349–2357.
- (22) Grondahl, L.; Chandler-Temple, A.; Trau, M. *Biomacromolecules* **2005**, *6*, 2197–2203.
- (23) Hu, S. G.; Jou, C. H.; Yang, M. C. *Biomaterials* **2003**, *24*, 2685–2693.
- (24) Wang, L. Y.; Wang, Y.-J.; Cao, D.-R. *J. Macromol. Sci.* **2009**, *46*, 765–773.
- (25) Zhu, Y.; Gao, C.; He, T.; Shen, J. *Biomaterials* **2004**, *25*, 423–430.
- (26) Xing, Z. C.; Chae, W. P.; Baek, J. Y.; Choi, M. J.; Jung, Y.; Kang, I. K. *Biomacromolecules* **2010**, *11*, 1248–1253.
- (27) Rossi, S.; Azghani, A. O.; Omri, A. *J. Antimicrob. Chemother.* **2004**, *54*, 1013–1018.

- (28) Sondi, I.; Salopek-Sondi, B. *J. Colloid Interface Sci.* **2004**, *275*, 177–182.
- (29) Alt, V.; Bechert, T.; Steinrucke, P.; Wagener, M.; Seidel, P.; Dingeldein, E.; Domann, E.; Schnettler, R. *Biomaterials* **2005**, *26*, 4383–4391.
- (30) Ramstedt, M.; Ekstrand-Hammarstrom, B.; Shchukarev, A.; Bucht, A.; Osterlund, I.; Welch, M.; Huck, W. *Biomaterials* **2009**, *30*, 1524–1531.
- (31) Flores, C. Y.; Minan, A. G.; Grillo, C. A.; Salvarezza, R. C.; Vericat, C.; Schilardi, P. L. *ACS Appl. Mater. Interfaces* **2013**, *5*, 3149–3159.
- (32) Elechiguerra, J.; Burt, J.; Monroe, J.; Camacho-Bragado, A.; Gao, X.; Lara, H. *J. Nanobiotechnol.* **2005**, *3* (6), 1–10.
- (33) Lacerda, S. H.; Park, J. J.; Meuse, C.; Pristinski, D.; Becker, M. L.; Karim, A.; Douglas, J. F. *ACS Nano* **2010**, *4*, 365–379.
- (34) Bhan, C.; Mandlewala, R.; Gabregeorgis, A.; Raghavan, D. *Langmuir* **2012**, *29*, 17043–17052.
- (35) Bhan, C.; Brower, T. L.; Raghavan, D. *J. Colloid Interface Sci.* **2013**, *402*, 40–49.
- (36) Lao, H. K.; Renard, E.; Linossier, I.; Langlois, V.; Vallee-Rehel, K. *Biomacromolecules* **2007**, *8*, 416–423.
- (37) Gebregeorgis, A.; Bhan, C.; Wilson, O.; Raghavan, D. *J. Colloid Interface Sci.* **2013**, *389*, 31–41.
- (38) Zhu, Y.; Gao, C.; Liu, X.; Shen, J. *Biomacromolecules* **2002**, *3*, 1312–1319.
- (39) Bradford, M. M. *Anal. Biochem.* **1976**, *72*, 248–259.
- (40) US EPA Contract Laboratory Program Statement of Work For Inorganic Analysis Multi-media Multi-concentration, USEPA 272.1 parts 4.1.1 through 4.1.3, pp D8–D12.
- (41) Keen, I.; Broota, P.; Rintoul, L.; Fredericks, P.; Trau, M.; Grondahl, L. *Biomacromolecules* **2006**, *7*, 427–434.
- (42) Hong, Y.; Gao, C.; Xie, Y.; Gong, Y.; Shen, J. *Biomaterials* **2005**, *26*, 6305–6313.
- (43) Lao, H.; Renard, E.; Langlois, V.; Vallee-Rehel, K.; Linossier, I. *J. Appl. Polym. Sci.* **2009**, *116*, 288–297.
- (44) Nguyen, S.; Yu, G.; Marchessault, R. H. *Biomacromolecules* **2002**, *3*, 219–224.
- (45) Liu, Q. S.; Zhu, M. F.; Wu, W. H.; Qin, Z. Y. *Polym. Degrad. Stab.* **2009**, *94*, 18–24.
- (46) Sestrem, R. H.; Ferreira, D. C.; Landers, R.; Temperini, M. L. A. *Eur. Polym. J.* **2010**, *46*, 484–493.
- (47) Hong, Y.; Gao, C.; Xie, Y.; Gong, Y.; Shen, J. *Biomaterials* **2005**, *26*, 6305–6313.
- (48) Mano, V.; Silva, M. E. *Mater. Res.* **2007**, *10*, 165–170.
- (49) Rodringues, F. T.; Martins, V. C. A.; Plepis, A. M. G. *Polímeros* **2010**, *20*, 92–97.
- (50) Bocking, T.; Kilian, K. A.; Hanley, T.; Ilyas, S.; Gaus, K.; Gal, M.; Gooding, J. J. *Langmuir* **2005**, *21*, 10522–10529.
- (51) Yan, T.; Sun, R.; Li, C.; Tan, B.; Mao, X.; Ao, N. *J. Mater. Sci.: Mater. Med.* **2010**, *21*, 2425–2433.
- (52) Xu, F. J.; Liu, L. Y.; Yang, W. T.; Kang, E. T.; Neoh, K. A. *Biomacromolecule* **2009**, *10*, 1665–1674.
- (53) Mohan, N.; Nair, P. D. *J. Biomed. Mater. Res.* **2008**, *84B*, 584–594.
- (54) Mariam, J.; Dongre, P. M.; Kothari, D. C. *J. Fluoresc.* **2011**, *21*, 2193–2199.
- (55) XiuJuan, S.; Dan, L.; Jing, X.; Shawn, W.; ZhaoQiang, W.; Hong, C. *Chin. Sci. Bull.* **2012**, *57*, 1109–1115.
- (56) Olde-Damink, L. H. H.; Dijkstra, P. J.; Van Luyn, M. J. A.; Van Wachem, P. B.; Nieuwenhuis, P.; Feijen, J. *Mater. Med.* **1995**, *6*, 460–472.